









# Effects of cold plasma treatment on the biological performances of decellularized bovine pericardium extracellular matrix-based films for biomedical applications

Maria Elena Lombardo<sup>1</sup> , Valentina Mariscotti<sup>1</sup>, Pascale Chevallier<sup>1</sup> , Francesco Copes<sup>1</sup> , Francesca Boccafoschi<sup>2,3</sup> , Andranik Sarkissian<sup>4</sup> , Diego Mantovani<sup>1\*</sup> 

<sup>1</sup>Laboratory for Biomaterials and Bioengineering, CRC-I, Department of Min-Met-Materials Engineering & CHU de Quebec Research Center, Division of Regenerative Medicine Laval, Laval University, Quebec City, QC G1V0A6, Canada

<sup>2</sup>TissueGraft Inc, 28100 Novara, Italy

<sup>3</sup>Department of Human Anatomy, Faculty of Medicine, University of Oriental Piedmont, 28100 Novara, Italy

<sup>4</sup>Plasmionique Inc, Varennes, QC J3X1S2, Canada

**\*Correspondence:** Diego Mantovani, Laboratory for Biomaterials and Bioengineering, CRC-I, Department of Min-Met-Materials Engineering & CHU de Quebec Research Center, Division of Regenerative Medicine Laval, Laval University, Quebec City, QC G1V0A6, Canada. [Diego.Mantovani@gmn.ulaval.ca](mailto:Diego.Mantovani@gmn.ulaval.ca)

**Academic Editor:** Tohid Didar, McMaster University, Canada

**Received:** October 25, 2023 **Accepted:** January 16, 2024 **Published:** April 23, 2024

**Cite this article:** Lombardo ME, Mariscotti V, Chevallier P, Copes F, Boccafoschi F, Sarkissian A, et al. Effects of cold plasma treatment on the biological performances of decellularized bovine pericardium extracellular matrix-based films for biomedical applications. *Explor BioMat-X*. 2024;1:84–99. <https://doi.org/10.37349/ebmx.2024.00007>

## Abstract

**Aim:** Since decades, decellularized extracellular matrix (dECM)-derived materials have received worldwide attention as promising biomaterials for tissue engineering and biomedical applications. Soluble dECM is a versatile raw material that can be easily engineered into the desired shapes and structures. However, there are still some limitations restricting its use, including low hydrophilicity and smooth surfaces, which negatively influence cell adhesion/spreading. The objective of the present study was to investigate surface modification by nitrogen/hydrogen (N<sub>2</sub>/H<sub>2</sub>) low-pressure cold plasma treatment as a potential technique to improve the biological response of bovine pericardium dECM films.

**Methods:** Bovine pericardium dECM was enzymatically digested and lyophilized prior to the preparation of thin films via solvent-casting method. Changes in surface properties after plasma treatment were investigated using water contact angle (WCA) and X-ray photoelectron spectroscopy (XPS) measurements. Immunofluorescence staining and resazurin assay for human dermal fibroblasts (HDFs) cultured on the dECM films were used to assess the bioactivity of dECM films. Finally, the hemocompatibility of the films was investigated via clotting time and hemolysis assay.

**Results:** WCA and XPS results revealed that oxygen (O)- and N-containing functional groups were incorporated onto the film surface and an increase in hydrophilicity was observed after plasma treatment. *In vitro* experiments showed that cell adhesion in plasma-treated dECM films is much faster if compared to the untreated controls. Moreover, the fibroblast proliferation increased after plasma surface modifications. Finally, the hemocompatibility analysis results indicated a delayed blood clotting and no hemolytic effects for all the tested samples.

© The Author(s) 2024. This is an Open Access article licensed under a Creative Commons Attribution 4.0 International License (<https://creativecommons.org/licenses/by/4.0/>), which permits unrestricted use, sharing, adaptation, distribution and reproduction in any medium or format, for any purpose, even commercially, as long as you give appropriate credit to the original author(s) and the source, provide a link to the Creative Commons license, and indicate if changes were made.



**Conclusions:** These findings confirmed the potential of dECM as raw material for biocompatible thin films fabrication. Additionally, plasma surface treatment emerged as an eco-friendly and cost-effective strategy to enhance *in vitro* cell attachment and proliferation on dECM films, expanding their applications in biomedicine.

## Keywords

Natural polymers, decellularized extracellular matrix, functionalization, low-pressure cold plasma, surface modifications, physicochemical properties, cell adhesion, hemocompatibility

---

## Introduction

During the last 20 years, growing evidence has supported the use of natural biomaterials derived from extracellular matrix (ECM) for a wide range of biomedical applications, from *in vitro* to *in vivo* preclinical animal studies up to human clinical trials [1]. The ECM represents a complex three-dimensional (3D) network of various macromolecules (such as collagens, elastin, glycosaminoglycans, proteoglycans, and glycoproteins), which provides a physical/mechanical support for cells with high impact on cell adhesion, proliferation and differentiation [2]. Moreover, ECM plays a critical role in numerous physiological activities including cell signaling, tissue growth, tissue remodelling, and homeostasis [3]. Decellularization is the process to isolate the ECM by removing antigenic cellular components from human or animal organs/tissues employing physical, chemical and/or enzymatic treatments while retaining the 3D structure, complex composition, physicochemical signals and biological performance of the natural ECM [4]. This allows to generate a 3D biomatrix [decellularized ECM (dECM)] with reduced risk of side effects upon implantation, such as inflammation and immune rejection [5]. One of the conventional methods of using dECM is as scaffold (tissue pieces or sections) that maintains its original macro- and micro-architecture and benefits. However, this limits dECM applications due to the highly specific scaffold geometries and difficulty to scale-down [6]. An alternative approach is to process dECM prior its utilization by the so called “post-decellularization processes”, including acidic enzymatic digestion and lyophilization, which make possible to break down the ECM structure and solubilize it into a liquid form [7]. These solutions can finally be used to obtain materials with more controllable physic-chemical properties, such as injectable hydrogels, electrospun films or bioinks for 3D printing and greatly expands the use dECM-derived biomaterials for both *in vitro* and *in vivo* applications [8]. Recently, dECM has also been explored for the production of thin films which can be applied as scaffolds for tissue regeneration [9] or coatings for metallic/polymeric surfaces [10]. Despite the preserved superior properties of dECM-based materials compared to other natural polymers to better mimic the *in vitro* natural cellular microenvironment [11], the steps involved in the post-decellularization process and the film fabrication method, such as the solvent-casting technique, can alter the initial dECM physic-chemical properties. This will lead to different cell-material interaction, different biological responses and finally diverse therapeutic efficacy [12].

As it is well known, one of the main drawbacks of developing thin films for biomedical applications is the presence of smooth surfaces characterized by low hydrophilicity and small pore sizes which inhibit a good cell adhesion and proliferation [13]. Cell adhesion on a surface represents the first important step in ensuring the survival of cells on a matrix, whether natural or synthetic [14]. In fact, this affects the subsequent cell expansion and differentiation, ensuring the success of a long-term implantation for each biomaterial and medical device [15]. Among the surface properties of any biomaterials, morphology, hydrophilicity, surface energy, and chemical composition play an important role in the interaction with the biological environment, particularly regarding cell attachment [16]. One of the traditional strategies to overcome the issue of an unresponsive material surfaces toward biological system interactions, is the surface modification, where the bulk properties of the material remain unchanged, while small alterations in the surface allow to obtain required characteristics [17]. During the years, numerous surface modification techniques have been developed to improve the bioactivity of biomaterials, by introducing a variety of reactive functional groups (usually polar groups) or bioactive compounds, mostly based on wet-

chemical methods. This classic approach involves the reaction between a surface and a chemical compound in a solution and can be performed in any laboratory environment since it does not require specialized equipment [18]. Unfortunately, these methods result being non-specific, not reproducible, and they generate hazardous chemical waste, cause degradation and irregular surface etching and may not be appropriate for larger scale applications [19]. Gas plasma surface treatments have emerged as a promising solvent-free and environmentally friendly alternative to wet-chemical methods [20] by significantly reducing the amount of the required organic solvents and the toxic waste products [21, 22]. Plasma can be described as a partially ionized gas composed of electrons, protons, and free radicals as well as reactive species and molecules with sufficient energy to interact with the material surface [23]. By tuning the plasma process parameters, such as type of inert gas, pressure, power, and treatment time, the surface chemistry of the treated material can be modulated in a controlled, reproducible and homogeneous way depending on the requirements and the particular applications [24]. For biomedical applications, plasma treatment has been used to improve the biocompatibility of surfaces by increasing the wettability of various polymer films, especially synthetic polymers [25–27], and with the incorporation of active functional groups, such as hydroxyl, carboxyl, aldehyde, or amine groups. This resulted into enhanced cell-adhesion properties and bioactivity [14, 28]. However, for natural polymers, only few reports have been proposed on plasma surface modification mostly aiming at improving cell-material interaction or to control the antibacterial activity or inflammatory response [29–32]. A further important requirement for biomaterials and their successful clinical applicability, especially for blood-contacting applications, is the hemocompatibility [33]. In general, surface modification by anticoagulants, such as heparin, albumin, or chitosan, together with surface covering with endothelial cells, have been utilized over many years to improve the hemocompatibility of both synthetic and natural polymer surfaces. However, all these methods need additional complex and expensive pre-treatment procedures, often involve chemicals difficult to completely remove, and a limited degree of success is often reported [34]. In the last years, low-pressure plasma surface modification has been considered as one of the promising methods to enhance the hemocompatibility of biomaterials. The procedure is generally rapid, in a dry environment, and samples do not need any specific pre-treatment before treatment [35].

In this challenging context, the goal of this study was to investigate if and how cold plasma-based surface modification of dECM thin films impacted their biological performances. Low-pressure cold plasma was applied to uniformly treat bovine pericardium dECM-based film surface. A nitrogen/hydrogen (N<sub>2</sub>/H<sub>2</sub>) blend was used as process gas due to the lower toxicity compared to traditional ammonia (NH<sub>3</sub>) gas and the well established cell adhesion promotion properties of N-rich plasma-treated polymer films [24, 26, 36, 37]. Physicochemical features of the dECM film (dECMf) surface, before and after plasma treatment, were investigated using X-ray photoelectron spectroscopy (XPS) analysis, contact angle measurements and tensile strength tests. Furthermore, fibroblasts *in vitro* attachment and proliferation on native and modified dECMfs were assessed as well as their hemocompatibility. So far, no studies were found in the current state-of-the-art on the effects of plasma treatment on dECM-based biopolymers and/or dECMfs in terms of bioactivity. The results validated the potential of processed decellularized bovine pericardium ECM as biomaterial for the preparation of thin films, and low-pressure cold-plasma treatment as suitable technique particularly indicated to improve their biological performances.

## Materials and methods

### Preparation and characterization of the dECMf

dECMfs were obtained using decellularized bovine pericardium kindly provided by Tissuegraft Srl (Novara, Piedmont, Italy; Italian patent number 10202000007567, patented on 29 April 2022; International patent number PCT/IB2021/052779 submitted on 2 April 2021) [38]. The films were prepared by a conventional solvent-casting method. Firstly, decellularized pericardia were enzymatically digested 10 mg/mL of milled dECM dissolved into 0.01 mol/L hydrochloric acid (HCl, cat# 320331, Sigma Aldrich, Oakville, ON, Canada) solution containing 1 mg/mL of pepsin from porcine gastric mucosa (cat# P7012, Sigma Aldrich, Oakville, ON, Canada) and then lyophilized to obtain dECM powder. For the film preparation, 1.2 g of the as-obtained

lyophilized dECM was added to 100 mL of 0.05 mol/L acetic acid and dissolved under constant stirring. This solution (4 mL) was then poured into a 37 mm diameter Teflon mold and the solvent left evaporated at room temperature in a home-made chamber using a dried-air flow for 12 h. Afterwards, the dried film was rinsed three times with deionized water and dried overnight at room temperature. The final obtained film was easy to peel off and approximately 50  $\mu\text{m}$  thick. Fourier-transform infrared spectroscopy (FTIR) was performed on the lyophilized dECM and dECMfs using a Cary 660 series (Agilent Technologies Inc., Santa Clara, California, USA) associated with an attenuated total reflectance block (GladiATR, Pikes Technologies Inc., Fitchburg, WI, USA). All the spectra were recorded in absorption mode from 400  $\text{cm}^{-1}$  to 4,000  $\text{cm}^{-1}$ . The background spectrum was subtracted and a baseline correction was performed.

### Low-pressure microwave plasma treatment

The plasma treatment on dECMfs was carried out by a microwave sourced low-pressure plasma system (Plasmionique Inc., Varennes, Quebec, Canada). The samples were placed in the chamber 5 cm from the plasma discharge region. The reactor chamber was first pumped down to a pressure below 1  $\mu\text{Torr}$  for 60 min. Subsequently, plasma was ignited at 100 kW using a pressure of 300 mTorr. Each sample was treated for 60 s on both the top and bottom sides using a combination of  $\text{N}_2$  and  $\text{H}_2$  as reactive gases ( $\text{N}_2:\text{H}_2$  pressure ratio 1:1). The plasma-treated dECMfs (dECMf\*) were directly used for all the tests afterwards. Untreated films were taken as controls.

### XPS analysis

The atomic chemical composition of untreated and dECMf\* surfaces was analyzed by XPS using a PHI 5600-ci equipment (Physical Electronics, Chanhassen, MN, USA), on an area of 500  $\mu\text{m}$  at a collecting angle of 45° with respect to the surface normal. A standard Al  $\text{K}\alpha$  (1,486.6 eV) X-ray source was used to record the survey spectra, while high resolution spectra of C1s, N1s and O1s were recorder with a standard Mg  $\text{K}\alpha$  X-ray source (1,253.6 eV). The charge referencing for all spectra was done by setting the C1s hydrocarbon peak at 285.00 eV. The curve fittings for high resolution XPS spectra were performed by employing Gaussian-Lorentzian functions, followed by subtraction of the Shirley-type background. Duplicate samples per each condition were analyzed.

### Contact angle measurement

The static water contact angle (WCA) of the dECMfs and dECMf\* was measured at room temperature by sessile drops technique, using a VCA optima XE (AST Products, Billerica, MA, USA) instrument. A drop of deionized water (0.5  $\mu\text{L}$ ) was deposited onto the surface. The contact angle was measured by image analysis with AutoFAST imaging software. For each film, at least five measurements on different locations were averaged and three replicates per condition were tested.

### Uniaxial tensile tests

Uniaxial tensile tests were performed on the samples using an Instron E1000 (Instron Corporation, Norwood, MA, USA) equipped with a 10 Newton load cell at room temperature. Tensile grips modified with rubber straps were employed to avoid sample slippage. The films were cut into a dog-bone shape of 1.25 cm wide and 3 cm long, with a narrowed central region approximately 0.85 cm wide and 0.75 cm long. The main thickness of each sample was measured in five different points by using a digital caliper to ensure uniformity. Specimens were subjected to uniaxial tension at a rate of 5 mm/min until rupture. Young's modulus (E) and ultimate tensile strength (UTS) were determined from stress-strain curves. These measurements were done in triplicate.

### *In vitro* cell culture

Human dermal fibroblasts (HDFs, cat# C0135C, Thermo-Fisher, Saint-Laurent, Quebec, Canada) were used in the following experiments. Briefly, HDFs were cultured in Dulbecco's modified Eagle's medium (DMEM, cat# 11965092, Gibco™, Invitrogen Corporation, Burlington, ON, Canada) with 10% fetal bovine serum (FBS, cat# 12483-020, Gibco™, Invitrogen Corporation, Burlington, ON, Canada), penicillin- streptomycin

(10,000 U/mL, cat# 15140122, Gibco™, Invitrogen Corporation, Burlington, ON, Canada). The cells were maintained at 37°C in a saturated atmosphere at 5% carbon dioxide (CO<sub>2</sub>). Media was changed every two days until a 90–95% confluence was reached. At this point, cells were detached from the plate using trypsin and then re-plated at a ratio of 1:5 or used for experiments. For the experiment hereby reported, cells have been used at passage 7.

### Cell adhesion and viability assay

In order to carry on the cell adhesion and viability tests, dECMfs and dECMf\* were previously prepared as follows. Briefly, both films were reduced to circular-shaped samples with a surface of about 0.8 cm<sup>2</sup> and transferred into a 48-well plate. After the sterilization under ultraviolet (UV) irradiation (wavelength 256 nm) for 1 h, the samples were rehydrated with sterilized deionized water three times. Thereafter, 300 µL of cellular suspension were kindly inoculated onto each sample to reach a seeding concentration of  $5 \times 10^4$  cells/cm<sup>2</sup>. The cell culture was conducted for up to 7 days.

To evaluate the cell adhesion on dECMfs, immunofluorescence staining was performed. HDFs have been seeded on samples for the different experimental conditions as previously described for the cell viability assay. After 6 h of incubation at 37°C in a saturated atmosphere at 5% CO<sub>2</sub>, cells have been fixed with 3.7% formaldehyde (cat# 252549, Sigma Aldrich, Oakville, ON, Canada) for 20 min. Afterwards, the fixed cells were permeabilized with 0.5% Triton X-100 (cat# T9284, Sigma Aldrich, Oakville, ON, Canada) and blocked with 3% bovine serum albumin (BSA, cat# A2153, Sigma Aldrich, Oakville, ON, Canada) in phosphate buffered saline (PBS, cat# P3813, Sigma Aldrich, Oakville, ON, Canada). Then cells have been incubated for 1 h at room temperature with rhodamine-conjugated phalloidin (1:200; cat# P1951, Sigma Aldrich, Oakville, ON, Canada) to stain the cells' actin filaments. Nuclei have been counter-stained with 4',6-diamidino-2-phenylindole (DAPI, cat# D3571, Invitrogen™ Thermo-Fisher Scientific, Saint-Laurent, Quebec, Canada). Afterwards, samples were placed on microscope slide for image acquisition. Images at a magnification of 20× have been collected using a Confocal Microscope (Zeiss NTS Ltd., White Plains, NY, USA).

Cell proliferation on dECMfs and dECMf\* was evaluated through a resazurin assay (cat# 199303, Millipore Sigma, Oakville, Canada). After 1 day, 3 days, and 7 days, the culture media was removed, and the cells were incubated for 4 h with a resazurin solution. Finally, the medium containing the produced resorufin was collected and fluorescence intensity (excitation wavelength of 545 nm and emission wavelength of 590 nm) was measured with a SpectraMax i3x Multi-Mode Plate Reader (Molecular Devices, San Jose, California, USA). The number of living cells is directly proportional to the fluorescence value. The cells cultured on the surface of tissue culture-treated plastic were used as control. The assay was carried out in triplicate for each time point.

### Hemocompatibility tests

To study the hemocompatibility of the dECMfs before and after plasma treatment, clotting time and hemolysis tests were carried out. Both tests were performed using whole human blood samples obtained from a healthy donor (CHU de Quebec ethic approval for human blood collection: SCH11-09-091). Blood samples were collected in sodium citrate tubes and used within 2 h from their collection. Circular-shaped dECMfs and dECMf\* (diameter = 1 cm and thick = 0.5 mm) were placed in a 24-well plate and sterilized on both sides by UV irradiation before testing. A triplicate for each condition was used.

For the clotting time test, 50 µL of citrated blood were added on the surface of each sterile sample. Tissue culture-treated plastic was used as control. After that, 10 µL of 0.1 mol/L calcium chloride (CaCl<sub>2</sub>, cat# 223506 Sigma Aldrich, Oakville, ON, Canada) were added to inhibit the anti-coagulant effect of the citrate and the samples were immediately incubated at 37°C for specific time points (0 min, 15 min, 30 min, 45 min, and 60 min). At the end of each time point, 1 mL of deionized water was added to each sample. The erythrocyte not entrapped in a blood clot were hemolyzed. One min later, the obtained solutions containing the free hemoglobin were aliquoted into a 96-well plate and the absorbance was measured at 540 nm using SpectraMax i3x Multi-Mode Plate Reader. Absorbance is proportional to the amount of free hemoglobin.

Therefore, the higher the absorbance, the higher the amount of free hemoglobin, the higher the hemocompatibility.

For the hemolysis test, the collected whole blood was first diluted in PBS 1× to a final ratio of 4:5 (4 parts of citrated blood and 5 parts of PBS 1×). In the meantime, each sample was pre-incubated in a 15 mL tube with 10 mL of PBS 1× at 37°C for 30 min. PBS 1× and deionized water were used as negative control and positive control, respectively. After the incubation time, 200 µL of diluted blood were added and mixed by carefully inverting each tube. At this point, samples and controls were incubated at 37°C for 1 h. Afterwards, the tubes were centrifuged at 800 *g* for 5 min. Supernatants containing red blood cell lysate were collected and 100 µL aliquots were placed in a 96-well plate. To measure released hemoglobin, the absorbance [optical density (OD)] at 540 nm was measured using a SpectraMax i3x Multi-Mode Plate Reader. The percentage of hemolysis was calculated according to the following equation:

$$\% \text{ Hemolysis} = \frac{OD_S - OD_{CTRLpos}}{OD_{CTRLpos} - OD_{CTRLneg}} \times 100$$

Where  $OD_S$  represents the absorbance of the sample analysed,  $OD_{CTRLpos}$  and  $OD_{CTRLneg}$  are the absorbance of the PBS 1× solution and the deionized water, respectively.

### Statistical analysis

All data generated in the experiments were reported as mean value ± standard deviation (SD). GraphPad software (Prism 10 Version 10.1.2) has been used for statistical analysis. For 2-group comparisons, an unpaired *t* test with Welch correction has been applied. To compare more than 2 groups, one-way analysis of variance (ANOVA) analysis followed by Tukey post-hoc test has been performed. Values of  $P < 0.05$  have been considered significant.

## Results

### FTIR analysis of dECM and dECMfs

FTIR spectra of the lyophilized dECM and dECMfs are shown in [Figure 1](#). Both spectra showed the typical peaks of type I collagen, such as a broad absorption band for amide A ( $3,318 \text{ cm}^{-1}$ ) and amide B ( $3,078 \text{ cm}^{-1}$ ), mainly associated with the stretching vibration of N-H groups [39, 40]. Moreover, it was possible to observe the strong peaks of amide I ( $1,648 \text{ cm}^{-1}$ ) and amide II ( $1,554 \text{ cm}^{-1}$ ) which are typical of proteins and correspond to the stretching vibration of C=O bonds and the N-H bending combined to C-N stretching vibrations, respectively. Finally, the amide III band was detected at  $1,236 \text{ cm}^{-1}$  which can be assigned to the C-N stretching, N-H bending vibrations and wagging vibrations of  $\text{CH}_2$  groups in the glycine backbone and proline side chains [41, 42].

### Chemical surface changes induced by plasma

Chemical changes on the treated dECMf surface were monitored by XPS analysis. As already mentioned, the most abundant protein in the dECM is collagen, which present a high percentage of oxygen (O) followed by N and carbon (C) [43]. The variation in the relative surface concentration of O, N, and C, together with N/C and O/C ratios of the untreated as well as the plasma-treated films, are shown in [Table 1](#). After  $\text{N}_2/\text{H}_2$  plasma treatment, an increase in the relative N content ( $13.1\% \pm 1.1\%$ ) and N/C ratio was observed, as expected. At the same time, the treated samples exhibited higher relative O content ( $20.3\% \pm 1.1\%$ ) and higher O/C ratio. The variation of chemical composition for the plasma-treated films was confirmed by peaks deconvolution of the XPS high resolution C1s spectra ([Figure 2](#)). In both treated and non-treated surfaces, three main peaks were identified at 285.0 eV, 286.4 eV and 288.1 eV which can be assigned to C-C/C-H, C-O/C-N and N-C=O bonds, respectively [37, 44]. Concerning the dECMf\*, a decrease in the C-C/C-H bond (from  $46.1\% \pm 2.8\%$  to  $36.6\% \pm 2.5\%$ ) has been compensated with an increase in the contribution of the amines C-N (from  $17.8\% \pm 2.2\%$  to  $21.2\% \pm 2.0\%$ ) and the amides -N-C=O (from  $10.4\% \pm 0.8\%$  to  $15.6\% \pm 1.05\%$ ) ([Figure 2B](#)).

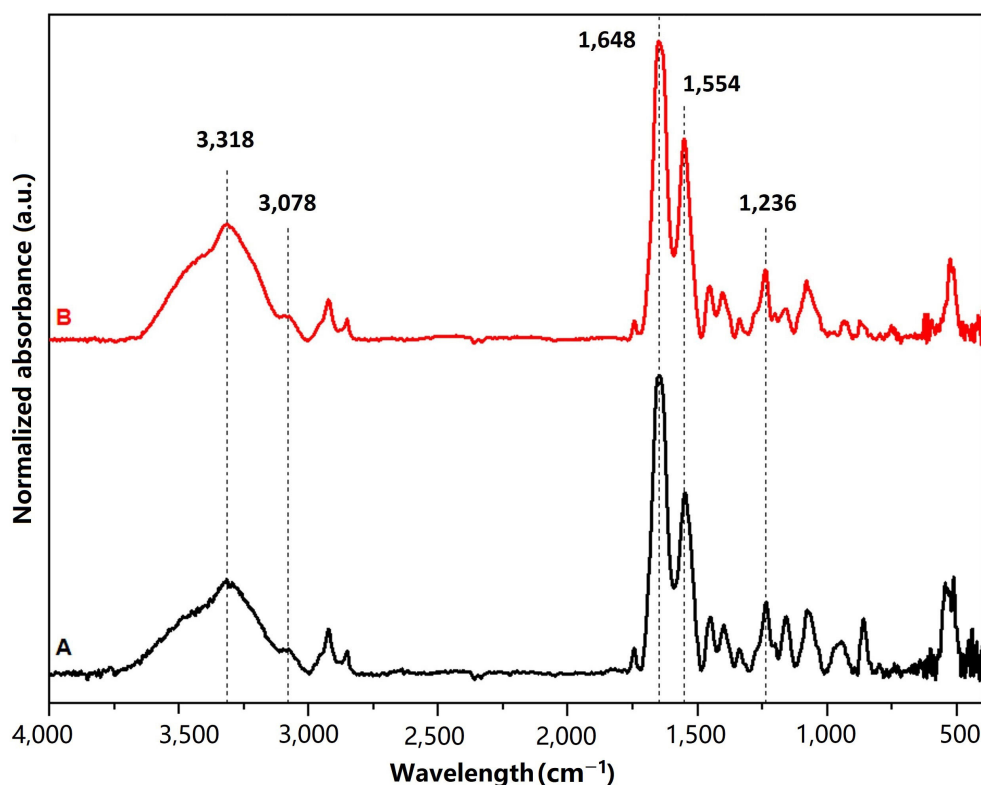


**Figure 1.** FTIR spectra. A. lyophilized dECM; B. dECMfs. a.u.: arbitrary unit

**Table 1.** Surface chemical composition obtained from XPS survey spectra and WCA of dECMf surface before and after plasma treatment

Sample	C (%)	O (%)	N (%)	N/C	O/C	WCA (°)
dECMfs	74.3 ± 0.7	15.5 ± 0.8	7.8 ± 0.6	0.11 ± 0.01	0.21 ± 0.01	92.4 ± 1.5
dECMf*	64.5 ± 1.9	20.3 ± 1.1	13.07 ± 1.1	0.20 ± 0.02	0.31 ± 0.03	86.1 ± 0.5

A statistically significant variation in the relative surface concentration of C ( $P = 0.0108$ ), O ( $P = 0.0111$ ) and N ( $P = 0.0225$ ) was observed. The WCA showed a significant decrease after plasma treatment ( $P < 0.0001$ ). Statistical analysis: unpaired  $t$  test with Welch correction

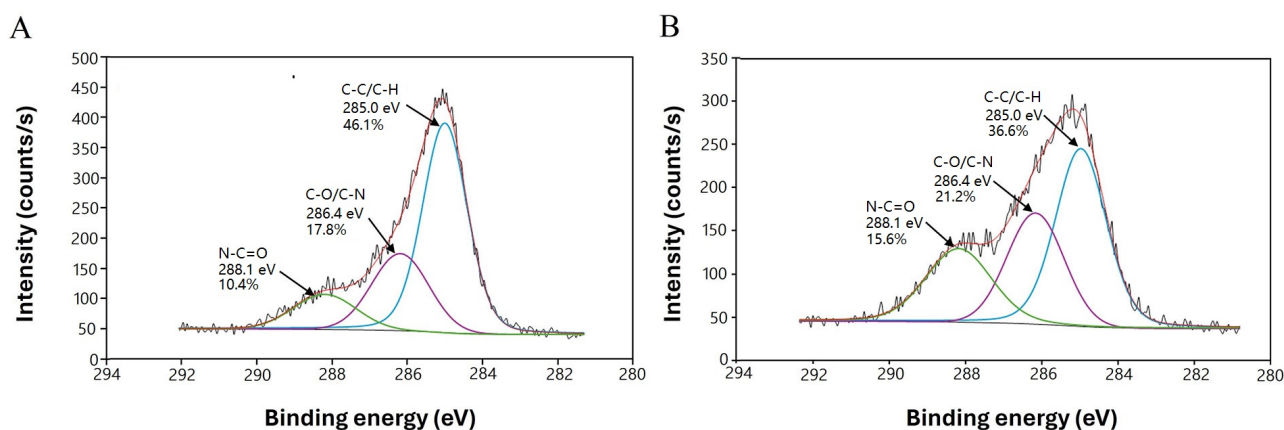


**Figure 2.** High-resolution C1s XPS spectrum. A. dECMfs; B. dECMf\*

### Effects of plasma on the hydrophilicity of dECMfs

The changes in hydrophilicity of the film surface after plasma treatment have been assessed using WCA measurement. As shown in Table 1, the WCA decreased significantly from  $92.4^\circ \pm 1.5^\circ$  in the untreated dECMfs to  $86.1^\circ \pm 0.5^\circ$  after  $N_2/H_2$  plasma treatment. Moreover, the obtained moderate hydrophilicity of the dECMf\* promoted a slow and moderate degradation of the samples after 28 days of incubation in PBS  $1\times$  solution at  $37^\circ C$  (data not shown).

### Evaluation of dECMfs stability and mechanical properties

The mechanical properties of treated and untreated dECMfs were evaluated. In Table 2, the UTS and E obtained from the stress-strain curves for both dECMfs and dECMf\* are reported. The data put into evidence that both the tensile strength and elastic modulus of the dECMf\*, resulted no different compared to the untreated films. Particularly, it was found that the untreated films showed a linear-elastic response with an E of 4.2 MPa ± 0.5 MPa, until an UTS of 17.9 MPa ± 4 MPa. Concerning the dECMf\*, a maximum UTS of 17.4 MPa ± 4 MPa and E of 4.4 MPa ± 0.5 MPa were recorded.

**Table 2.** Mechanical properties of untreated and dECMf\*

Sample	UTS (MPa)	E (MPa)
dECMfs	17.9 ± 4	4.2 ± 0.5
dECMf*	17.6 ± 4	4.4 ± 0.5

No difference was observed for UTS ( $P = 0.0255$ ) and E [ $P = 0.7017$  non-significance (ns)]. Statistical analysis: unpaired *t* test with Welch correction

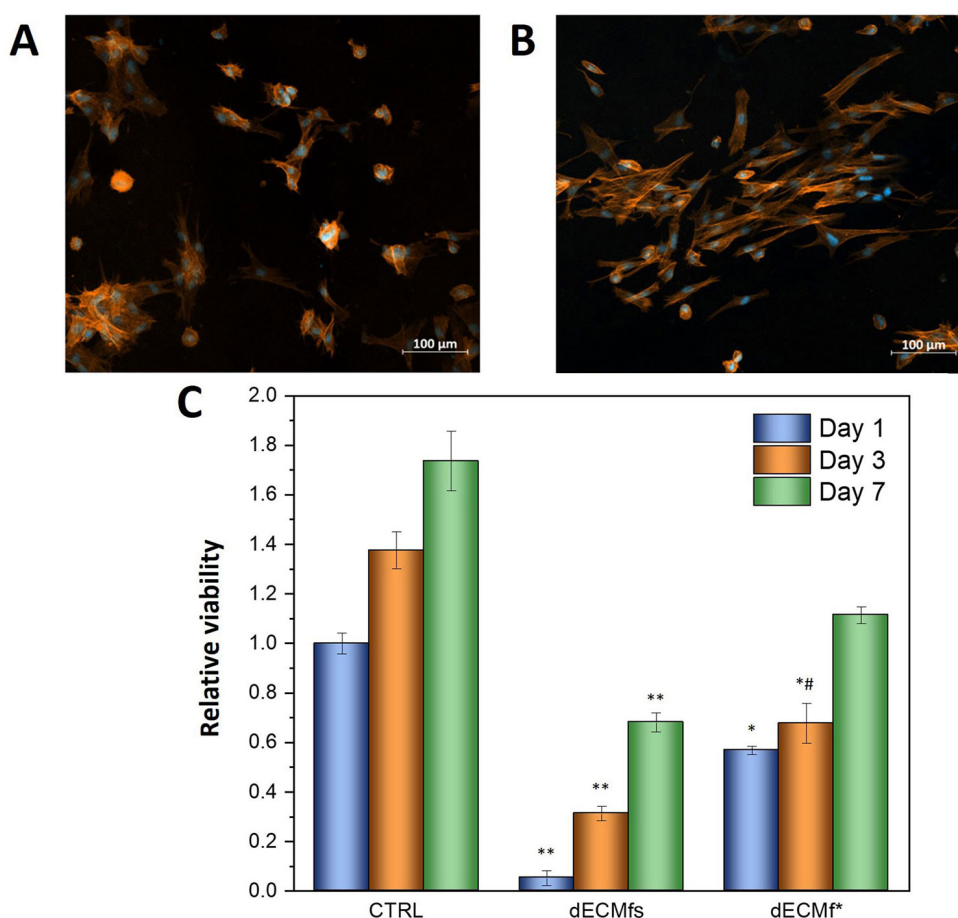


**Figure 3.** Biological characterizations of dECMfs and dECMf\*. A, B. Confocal microscopy images of DAPI and rhodamine/phalloidin staining HDFs after 6 h of incubation at 37°C on dECMfs and dECMf\* respectively. Cell nuclei stained with DAPI appear in blue; actin filaments of cytoplasm stained with rhodamine-phalloidin appear in red. C. Cell viability evaluated by resazurin assay after culturing HDFs on dECMfs and dECMf\* for 1 day, 3 days and 7 days. \*  $P < 0.05$ , \*\*  $P < 0.0001$  significant differences compared with cell-culture plastic control (CTRL); #  $P < 0.05$  significant differences between dECMfs and dECMf\*. CTRL vs. dECMfs: day 1, 3, and 7,  $P < 0.0001$ . CTRL vs. dECMf\*: day 1,  $P = 0.0205$ ; day 3,  $P = 0.0484$ ; day 7,  $P = 0.0664$ , non-significance (ns). ECM vs. dECMf\*: day 1,  $P = 0.1313$ , ns; day 3,  $P = 0.0484$ ; day 7,  $P = 0.0664$ , ns. Statistical analysis: ANOVA followed by Tukey post-hoc test

### Cell behavior on dECMfs after N<sub>2</sub>/H<sub>2</sub> plasma treatment

HDFs adhesion onto the untreated and dECMf\* was investigated by analyzing confocal micrographs of DAPI/rhodamine-phalloidin stained cells. The images were captured after 6 h of culture at 37°C and 5% CO<sub>2</sub>. As can be observed in Figure 3A and 3B, cells were able to adhere on both substrates. However, despite the presence of few cells on the control film (untreated surface) showing an elongated phenotype, the



majority of the seeded HDFs show a phenotype referable to an early-stage cell adhesion (Figure 3A). On the contrary, Figure 3B shows more cells with an elongated, spindle-like shape, typical for fibroblast cells, for the dECMf\*.

Comparable results were obtained by cytocompatibility tests and are shown in Figure 3C. HDFs viability on dECMfs and dECMf\* was evaluated after 1 day, 3 days and 7 days after seeding using a resazurin assay. Cell proliferation on both samples was clearly reduced compared to the CTRL. However, higher cell viability was observed on dECMf\* on day 1 compared to the untreated dECMf. This is in accordance with the results observed for the adhesion test. In addition, the cell proliferation rate on dECMf\* remained remarkably higher than dECMfs from day 1 to day 7.

### Effect of plasma on dECMf hemocompatibility

The anticoagulant activity of dECM and dECMf\* has been evaluated using the clotting time. The whole human blood was allowed to clot up to 60 min on all the surfaces, and the amount of free hemoglobin released after addition of deionized water, was measured every 15 min (Figure 4A). As expected, at time point “0 min” the blood did not coagulate for both the conditions tested. Therefore, this value was considered as maximal hemocompatibility and used as reference for further time points. Both untreated and treated films showed a higher anticoagulant activity than the plastic control for all the time points analyzed. Additionally, dECMf\* showed a higher hemocompatibility compared with the untreated film after 15 min and 30 min of incubation, even if not statistically significant. On the contrary, no significant differences were observed between dECMfs and dECMf\* for the next two time points (45 min and 60 min).

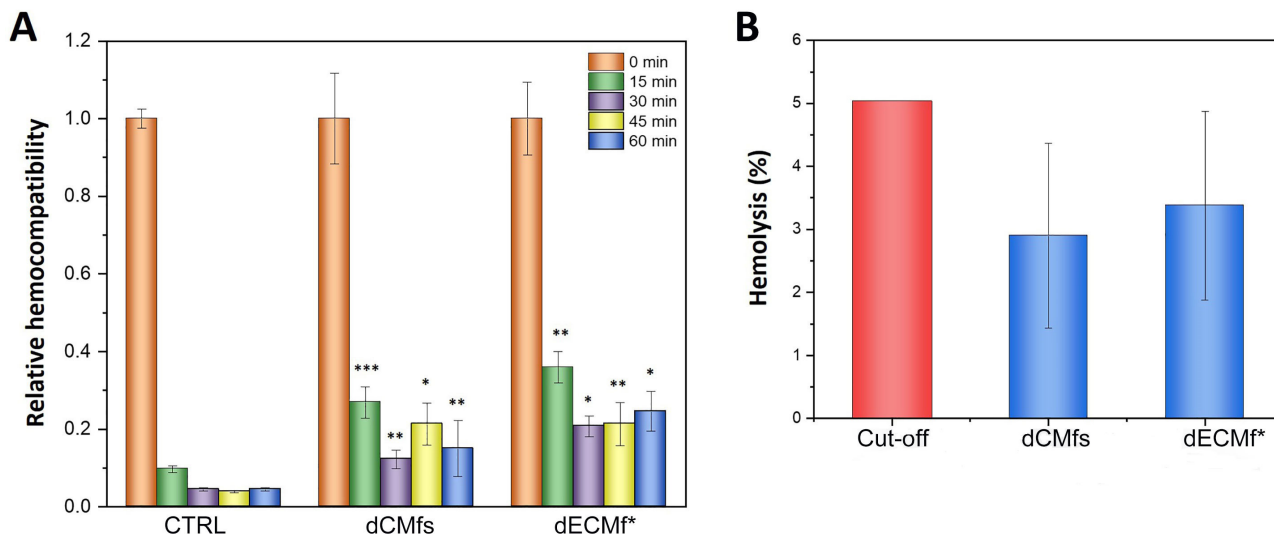


**Figure 4.** Hemocompatibility tests. A. Relative hemocompatibility of dECMfs and dECMf\* in contact with whole human blood from clotting time tests at 0 min, 15 min, 30 min, 45 min, and 60 min; B. hemolysis of dECMfs and dECMf\* in contact with whole human blood for 1 h. Cut-off: critical hemolysis value outlined in the standard practice for assessment of hemolytic properties of materials (ASTM F756) standard for assessment of hemolytic properties of materials. \*  $P < 0.05$ , \*\*  $P < 0.01$ , \*\*\*  $P < 0.0001$  significant differences compared with CTRL. CTRL vs. dECMfs: 15 min,  $P < 0.0001$ ; 30 min,  $P = 0.0042$ ; 45 min,  $P < 0.0001$ ; 60 min,  $P = 0.0003$ . CTRL vs. dECMf\*: 15 min,  $P = 0.0029$ ; 30 min,  $P < 0.0001$ ; 45 min,  $P = 0.0021$ ; 60 min,  $P < 0.0001$ . dECMfs vs. dECMf\*: 15 min,  $P > 0.9999$  non-significance (ns); 30 min,  $P = 0.9922$  ns; 45 min,  $P = 0.2395$  ns; 60 min,  $P > 0.9999$  ns. Statistical analysis: ANOVA followed by Tukey post-hoc test

The hemocompatibility of the samples was also evaluated using the hemolysis test which measures the ability of a material to cause rupture of red blood cells. The graph in Figure 4B shows the hemolysis assay after exposing dECMfs to whole human blood for 1 h at 37°C. Both the untreated and plasma-treated films showed a percentage of hemolysis lower than the 5% threshold, which is the critical hemolysis value outlined in the ASTM F756 standard for assessment of hemolytic properties of materials [45].

## Discussion

The dECMfs used in this study were obtained by solvent-casting method of lyophilized-digested bovine pericardium dECM. As reported in a previous study [46], the as-mentioned bovine pericardium dECM is mainly composed of type I collagen (approximately 90%). Since film preparation methods could affect dECM final properties including structure, physicochemical and mechanical characteristics [12], FTIR spectroscopy was performed to determine whether the native dECM composition persists after the film preparation. The obtained spectra (Figure 1) were comparable and displayed the typical bands of type I collagen, including amide A and amide B, amide I, II and III (Figure 1). As reported in literature, the presence of the amide bands in the infrared (IR) spectra confirmed an intact triple-helical structure of type I collagen [39] despite the film preparation.

To monitor the effects of N<sub>2</sub>/H<sub>2</sub> low-pressure plasma treatment on chemical and physical properties of dECMfs, various analysis have been conducted in this work.

The incorporation of functional groups on the plasma-treated films was identified using XPS analysis. At first, an increase in the relative N content and N/C ratio was observed (Table 1). In fact, as reported in literature, N-rich plasmas, such as N<sub>2</sub> and NH<sub>3</sub> plasmas, are primarily applied for the incorporation of N on polymeric surfaces [47, 48]. In addition, the dECMf\* showed higher relative O content and higher O/C ratio (Table 1). The presence of O after non-O plasma treatments is a common phenomenon. This can be explained by the interaction of the treated samples with the ambient wet air during the sample storage. In particular, the free radicals and high react species generated by the plasma treatment act as the basis for certain reactions with O<sub>2</sub> and water vapor which induce a post-plasma functionalization [49]. Furthermore, the results of peaks deconvolution of the XPS high resolution C1s spectra (Figure 2) may explain the aforementioned increase in the N/C ratio after N-rich plasma treatment. In numerous works in literature, the same functionalization (N-containing and O-containing functional groups) on natural polymeric films, including cellulose-based [50], chitosan-based [51] and collagen-based films [29], is reported after N-rich plasma treatments.

One of the most important factors determining cell-material interaction is surface wettability [52]. Commonly, a moderate wettability (between 10° and 90°) is preferred [53] since both super-hydrophilicity (WCA < 2°) and super-hydrophobicity (WCA > 150°) are not favorable conditions for cell adhesion and proliferation on polymeric surfaces [54]. In this study, an increased hydrophilicity has been observed in the plasma-treated samples (Table 1), as expected, according to the insertion of both N- and O-containing functional groups on the surface. In fact, it is well-known that the presence on polymeric surfaces of both polar groups [47, 55] plays a key role in improving the wettability. These results can guarantee good cell-polymer interactions suitable for further *in vitro* and *in vivo* applications [56].

In the design of engineered biomaterials, mechanical characteristics is one of the important aspects to consider for their applications in any biomedical science [57]. Hence in this work, the influence of plasma treatment on the tensile strength of the dECMfs was evaluated. Particularly, UTS and E were investigated. A non-statistically significant difference has been recorded between the dECMfs and the dECMf\* for both UTS and E data (Table 2). This is in accordance with some studies, where N<sub>2</sub> cold-plasma treatment had no considerable effects on the bulk mechanical properties of polymeric films based on natural [58] or synthetic polymers [59].

A delayed adhesion of HDFs has been observed in the confocal image of the untreated films (Figure 3A) which corresponded to a lower cell viability after 24 h of culture. By contrast, the promoted cell adhesion after 6 h of seeding on the plasma-treated films (Figure 3B) leads to increased cell growth on the plasma-treated films for all the 7 days of culture (Figure 3C). These results were similar to the reported literature, where the hydrophilicity and high polarity of the polymeric surfaces using different plasma treatments were recognized as optimal way to regulate cell-biomaterial interactions [60]. Particularly, the incorporation by plasma of N-containing groups, such as amine and amide, plays an important role for cell adhesion and growth. One advantage may be the positive charge of a fraction of them at the physiological pH, which promotes cell-material interaction due to the negative charge of cell membrane. In their work,

Yang et al. [61] examined the adhesion and proliferation of mouse 3T3 fibroblast cells on NH<sub>3</sub> plasma-treated poly-D, L-lactic acid (PDLLA) films. After 4 days of culture, plasma modified surfaces yielded a higher number of cells attached and a faster rate of growth compared to the untreated control films. Recently, Davoodi et al. [62] demonstrated that by applying O<sub>2</sub> and N<sub>2</sub> low-pressure, non-thermal plasma on poly-lactic acid (PLA) films, fibroblast cells (L929) tended to better attach, spread and migrate across the treated surface. Considering natural polymer, an interesting work of Prasertsung et al. [63] showed how N<sub>2</sub> plasma can modify the surface of gelatin films and influence the behavior of two different cell lines (mouse fibroblast L929 and rat bone marrow-derived mesenchymal stem cell (MSC)). Both cells exhibited greater adhesion and proliferation on the treated surfaces compared to the untreated surfaces.

Finally, dECMfs showed good hemocompatibility results in terms of blood coagulation risk and hemolysis percentage before and after plasma treatment. Particularly, the results of clotting time test suggested that the blood clotting was delayed on dECM plasma-treated surfaces, which is comparable to what other authors observed for plasma-treated synthetic polymers, such as, PLA, polycaprolactone (PCL) and polyethylene (PE), using O<sub>2</sub>, argon (Ar), N<sub>2</sub> or NH<sub>3</sub> as gases [64, 65]. As it is well known, collagen is the main component of ECM and one of the major proteins involved in initiating hemostasis when in contact with flowing blood [66]. Therefore, in clinical treatments, collagen is often combined with anticoagulants, such as heparin [67] or hyaluronic acid [68], to regulate its thrombogenic activity. In the present study, plasma surface treatment allowed to modify the surface of dECMfs with an enhanced hemocompatibility activity using a one-step procedure and avoiding the addition of secondary macromolecules. These preliminary findings show the potential of plasma-treated dECM materials for future clinical applications also involving material-blood contact.

In conclusion, dECM-based biomaterials have recently emerged as an ideal platform for tissue engineering and biomedical applications especially due to the unique biological advantages compared to other natural polymers [69]. However, there are still several key limitations that will need to be overcome in order to expand their future applications, including optimization of dECM final forms and bioactivity after post-decellularization processes [70]. In the present study, surface modification by low-pressure N<sub>2</sub>/H<sub>2</sub> cold-plasma treatment was successfully used to improve cell-material interaction of bovine pericardium dECM-based films. The plasma treatment did not affect the bulk properties, as tensile strength, of the film resulting very close to the unmodified one. Due to the presence of new polar functional groups, such as C-O/C-N bond and -N-C=O amide groups, and higher surface wettability, fibroblast cells cultured on such plasma-modified dECMfs exhibited faster adhesion and improved proliferation compared to the unmodified films. As mentioned above, the decellularized bovine pericardium used in this work for the dECMf preparation is mostly made of type I collagen [46]. It is well known that one of the major problems of collagen-based surfaces is the intrinsic thrombogenicity which limits their clinic applications [71]. The experimental results obtained in this study revealed interesting hemocompatible properties for both untreated and dECMf\*. To conclude, this preliminary work confirms the potential of the dECM as a valid alternative biomaterial to the traditional synthetic and natural polymers for films preparation. Moreover, it opens the door to future research of the low-pressure cold-plasma process as an effective and environmentally friendly surface treatment for improving dECMf bioactivity and expand their applications for biological and medical research.

## Abbreviations

3D: three-dimensional

ANOVA: analysis of variance

C: carbon

CO<sub>2</sub>: carbon dioxide

CTRL: cell-culture plastic control

DAPI: 4',6-diamidino-2-phenylindole  
dECM: decellularized extracellular matrix  
dECM<sup>f</sup>: plasma-treated decellularized extracellular matrix films  
dECM<sub>f</sub>: decellularized extracellular matrix film  
E: Young's modulus  
ECM: extracellular matrix  
FTIR: Fourier-transform infrared spectroscopy  
H<sub>2</sub>: hydrogen  
HDFs: human dermal fibroblasts  
N<sub>2</sub>: nitrogen  
NH<sub>3</sub>: ammonia  
O: oxygen  
OD: optical density  
PBS: phosphate buffered saline  
UTS: ultimate tensile strength  
WCA: water contact angle  
XPS: X-ray photoelectron spectroscopy

## Declarations

### Author contributions

MEL: Conceptualization, Data curation, Formal analysis, Investigation, Writing—original draft, Writing—review & editing. VM: Conceptualization, Data curation, Investigation. PC and FC: Conceptualization, Supervision, Validation, Writing—review & editing. FB and AS: Conceptualization, Project administration, Resources, Validation, Writing—review & editing. DM: Conceptualization, Funding acquisition, Project administration, Resources, Validation, Writing—review & editing. All authors have read and agreed to the published version of the manuscript.

### Conflicts of interest

The authors declare that they have no conflicts of interest.

### Ethical approval

This study was approved by the CHU de Quebec ethic (SCH11-09-091). This study complies with the WMA Declaration of Helsinki.

### Consent to participate

Not applicable.

### Consent to publication

Not applicable.

### Availability of data and materials

The data supporting the conclusions of this study will be made available by the corresponding author on request.

## Funding

This work was partially supported by the Natural Science and Engineering Research Council of Canada, the Ministry of Economy and Innovation of Quebec (PRIMA Quebec), and the Research Center of the CHU de Quebec. The funders had no role in study design, data collection and analysis, decision to publish, or preparation of the manuscript.

## Copyright

© The Author(s) 2024.

## References

1. Hernandez MJ, Yakutis GE, Zelus EI, Hill RC, Dzieciatkowska M, Hansen KC, et al. Manufacturing considerations for producing and assessing decellularized extracellular matrix hydrogels. *Methods*. 2020;171:20–7.
2. McInnes AD, Moser MAJ, Chen X. Preparation and use of decellularized extracellular matrix for tissue engineering. *J Funct Biomater*. 2022;13:240.
3. Yao Q, Zheng YW, Lan QH, Kou L, Xu HL, Zhao YZ. Recent development and biomedical applications of decellularized extracellular matrix biomaterials. *Mater Sci Eng C*. 2019;104:109942.
4. Amirazad H, Dadashpour M, Zarghami N. Application of decellularized bone matrix as a bioscaffold in bone tissue engineering. *J Biol Eng*. 2022;16:1.
5. Koo MA, Jeong H, Hong SH, Seon GM, Lee MH, Park JC. Preconditioning process for dermal tissue decellularization using electroporation with sonication. *Regen Biomater*. 2022;9:rbab071.
6. Kim YS, Majid M, Melchiorri AJ, Mikos AG. Applications of decellularized extracellular matrix in bone and cartilage tissue engineering. *Bioeng Transl Med*. 2018;4:83–95.
7. Bejleri D, Davis ME. Decellularized extracellular matrix materials for cardiac repair and regeneration. *Adv Healthc Mater*. 2019;8:e1801217.
8. Saldin LT, Cramer MC, Velankar SS, White LJ, Badylak SF. Extracellular matrix hydrogels from decellularized tissues: structure and function. *Acta Bioma*. 2017;49:1–15.
9. Arslan YE, Galata YF, Sezgin Arslan T, Derkus B. Trans-differentiation of human adipose-derived mesenchymal stem cells into cardiomyocyte-like cells on decellularized bovine myocardial extracellular matrix-based films. *J Mater Sci Mater Med*. 2018;29:127.
10. Liao J, Xu B, Zhang R, Fan Y, Xie H, Li X. Applications of decellularized materials in tissue engineering: advantages, drawbacks and current improvements, and future perspectives. *J Mater Chem B*. 2020;8:10023–49.
11. Yao S, Cui J, Chen S, Zhou X, Li J, Zhang K. Extracellular matrix coatings on cardiovascular materials—a review. *Coatings*. 2022;12:1039.
12. Efraim Y, Schoen B, Zahran S, Davidov T, Vasilyev G, Baruch L, et al. 3D structure and processing methods direct the biological attributes of ECM-based cardiac scaffolds. *Sci Rep*. 2019;9:5578.
13. Cai S, Xu H, Jiang Q, Yang Y. Novel 3D electrospun scaffolds with fibers oriented randomly and evenly in three dimensions to closely mimic the unique architectures of extracellular matrices in soft tissues: fabrication and mechanism study. *Langmuir*. 2013;29:2311–8.
14. Cai S, Wu C, Yang W, Liang W, Yu H, Liu L. Recent advance in surface modification for regulating cell adhesion and behaviors. *Nanotechnol Rev*. 2020;9:971–89.
15. Firoozi M, Entezam M, Masaeli E, Ejeian F, Nasr-Esfahani MH. Physical modification approaches to enhance cell supporting potential of poly (vinyl alcohol)-based hydrogels. *J Appl Polym Sci*. 2022;139:51485.
16. López-Pérez PM, Marques AP, da Silva RMP, Pashkuleva I, Reis RL. Effect of chitosan membrane surface modification via plasma induced polymerization on the adhesion of osteoblast-like cells. *J Mater Chem*. 2007;17:4064–71.

17. Klee D, Ademovic Z, Bosserhoff A, Hoecker H, Maziolis G, Erli HJ. Surface modification of poly(vinylidene fluoride) to improve the osteoblast adhesion. *Biomaterials*. 2003;24:3663–70.
18. Goddard JM, Hotchkiss JH. Polymer surface modification for the attachment of bioactive compounds. *Prog Polym Sci*. 2007;32:698–725.
19. Barish JA, Goddard JM. Topographical and chemical characterization of polymer surfaces modified by physical and chemical processes. *J Appl Polym Sci*. 2011;120:2863–71.
20. Yoshida S, Hagiwara K, Hasebe T, Hotta A. Surface modification of polymers by plasma treatments for the enhancement of biocompatibility and controlled drug release. *Surf Coatings Technol*. 2013;233:99–107.
21. Vaz JM, Taketa TB, Hernandez-Montelongo J, Chevallier P, Cotta MA, Mantovani D, et al. Antibacterial properties of chitosan-based coatings are affected by spacer-length and molecular weight. *Appl Surf Sci*. 2018;445:478–87.
22. Ma C, Nikiforov A, De Geyter N, Morent R, Ostrikov KK. Plasma for biomedical decontamination: from plasma-engineered to plasma-active antimicrobial surfaces. *Curr Opin Chem Eng*. 2022;36:100764.
23. Valence Sd, Tille JC, Chaabane C, Gurny R, Bochaton-Piallat ML, Walpoth BH, et al. Plasma treatment for improving cell biocompatibility of a biodegradable polymer scaffold for vascular graft applications. *Eur J Pharm Biopharm*. 2013;85:78–86.
24. Ino JM, Chevallier P, Letourneur D, Mantovani D, Le Visage C. Plasma functionalization of poly(vinyl alcohol) hydrogel for cell adhesion enhancement. *Biomatter*. 2013;3:e25414.
25. Cámara-Torres M, Sinha R, Scopece P, Neubert T, Lachmann K, Patelli A, et al. Tuning cell behavior on 3D scaffolds fabricated by atmospheric plasma-assisted additive manufacturing. *ACS Appl Mater Interfaces*. 2021;13:3631–44.
26. Turkoglu Sasmazel H, Alazzawi M, Kadim Abid Alsaheb N. Atmospheric pressure plasma surface treatment of polymers and influence on cell cultivation. *Molecules*. 2021;26:1665.
27. Maryin PV, Tran TH, Frolova AA, Buldakov MA, Choinzonov EL, Kozelskaya AI, et al. Electrospun poly-L-lactic acid scaffolds surface-modified via reactive magnetron sputtering using different mixing ratios of nitrogen and xenon. *Polymers (Basel)*. 2023;15:2969.
28. Eswaramoorthy N, McKenzie DR. Plasma treatments of dressings for wound healing: a review. *Biophys Rev*. 2017;9:895–917.
29. García JL, Asadinezhad A, Pacherník J, Lehocký M, Junkar I, Humpolíček P, et al. Cell proliferation of HaCaT keratinocytes on collagen films modified by argon plasma treatment. *Molecules*. 2010;15:2845–56.
30. Taraballi F, Zanini S, Lupo C, Panseri S, Cunha C, Riccardi C, et al. Amino and carboxyl plasma functionalization of collagen films for tissue engineering applications. *J Colloid Interface Sci*. 2013;394:590–7.
31. Chen R, Curran J, Pu F, Zhuola Z, Bayon Y, Hunt JA. *In vitro* response of human peripheral blood mononuclear cells (PBMC) to collagen films treated with cold plasma. *Polymers (Basel)*. 2017;9:254.
32. Demina TS, Bikmulina PY, Birdibekova AV, Kuryanova AS, Frolova AA, Koteneva PI, et al. Modification of the chemical structure, morphology, and cytocompatibility of chitosan films via low-frequency plasma treatment. *Appl Biochem Microbiol*. 2022;58:118–25.
33. Weber M, Steinle H, Golombek S, Hann L, Schlensak C, Wendel HP, et al. Blood-contacting biomaterials: *in vitro* evaluation of the hemocompatibility. *Front Bioeng Biotechnol*. 2018;6:99.
34. Wilson DJ, Rhodes NP, Williams RL. Surface modification of a segmented polyetherurethane using a low-powered gas plasma and its influence on the activation of the coagulation system. *Biomaterials*. 2003;24:5069–81.
35. Recek N. Biocompatibility of plasma-treated polymeric implants. *Materials (Basel)*. 2019;12:240.

36. Lopez LC, Belviso MR, Gristina R, Nardulli M, d'Agostino R, Favia P. Plasma-treated nitrogen-containing surfaces for cell adhesion: the role of the polymeric substrate. *Plasma Process Polym.* 2007;4:S402–5.
37. Truica-Marasescu F, Wertheimer MR. Nitrogen-rich plasma-polymer films for biomedical applications. *Plasma Process Polym.* 2008;5:44–57.
38. Boccafoschi F, Calvo Catoira M, Fusaro L, inventors. Hydrogel from bovine pericardium for medical use. International application PCT/IB2021/052779. 2 April 2021.
39. Hu Y, Liu L, Gu Z, Dan W, Dan N, Yu X. Modification of collagen with a natural derived cross-linker, alginate dialdehyde. *Carbohydr Polym.* 2014;102:324–32.
40. Riaz T, Zeeshan R, Zarif F, Ilyas K, Muhammad N, Safi SZ, et al. FTIR analysis of natural and synthetic collagen. *Appl Spectrosc Rev.* 2018;53:703–46.
41. Sanden KW, Kohler A, Afseth NK, Böcker U, Rønning SB, Liland KH, et al. The use of fourier-transform infrared spectroscopy to characterize connective tissue components in skeletal muscle of Atlantic cod (*Gadus morhua* L.). *J Biophotonics.* 2019;12:e201800436.
42. Huang CC. Microporous scaffolds via a designed decellularization procedure combined with papain-containing reagent treatments after supercritical fluid of carbon dioxide. *Mater Lett.* 2021;304:130539.
43. Naomi R, Ridzuan PM, Bahari H. Current insights into collagen type I. *Polymers (Basel).* 2021;13:2642.
44. Wang MJ, Chang YI, Poncin-Epaillard F. Effects of the addition of hydrogen in the nitrogen cold plasma: the surface modification of polystyrene. *Langmuir.* 2003;19:8325–30.
45. Loffredo S, Gambaro S, Copes F, Paternoster C, Giguère N, Vedani M, et al. Effect of silver in thermal treatments of Fe-Mn-C degradable metals: implications for stent processing. *Bioact Mater.* 2022;12:30–41.
46. Di Francesco D, Bertani F, Fusaro L, Clemente N, Carton F, Talmon M, et al. Regenerative potential of a bovine ECM-derived hydrogel for biomedical applications. *Biomolecules.* 2022;12:1222.
47. Kull KR, Steen ML, Fisher ER. Surface modification with nitrogen-containing plasmas to produce hydrophilic, low-fouling membranes. *J Memb Sci.* 2005;246:203–15.
48. López-Santos C, Yubero F, Cotrino J, González-Elipe AR. Nitrogen plasma functionalization of low density polyethylene. *Surf Coatings Technol.* 2011;205:3356–64.
49. Sanchis MR, Calvo O, Fenollar O, Garcia D, Balart R. Characterization of the surface changes and the aging effects of low-pressure nitrogen plasma treatment in a polyurethane film. *Polym Test.* 2008;27:75–83.
50. Kawano T, Wang MJ, Andou Y. Surface modification of a regenerated cellulose film using low-pressure plasma treatment with various reactive gases. *ACS Omega.* 2022;7:44085–92.
51. Luna SM, Silva SS, Gomes ME, Mano JF, Reis RL. Cell adhesion and proliferation onto chitosan-based membranes treated by plasma surface modification. *J Biomater Appl.* 2011;26:101–16.
52. Arima Y, Iwata H. Effect of wettability and surface functional groups on protein adsorption and cell adhesion using well-defined mixed self-assembled monolayers. *Biomaterials.* 2007;28:3074–82.
53. Samanta A, Wang Q, Shaw SK, Ding H. Roles of chemistry modification for laser textured metal alloys to achieve extreme surface wetting behaviors. *Mater Des.* 2020;192:108744.
54. Majhy B, Priyadarshini P, Sen AK. Effect of surface energy and roughness on cell adhesion and growth – facile surface modification for enhanced cell cultur. *RSC Adv.* 2021;11:15467–76.
55. Bismarck A, Brostow W, Chiu R, Hagg Lobland HE, Ho KKC. Effects of surface plasma treatment on tribology of thermoplastic polymers. *Polym Eng Sci.* 2008;48:1971–6.
56. Chen L, Yan C, Zheng Z. Functional polymer surfaces for controlling cell behaviors. *Mater Today.* 2018;21:38–59.
57. Bharadwaj A. An overview on biomaterials and its applications in medical science. *IOP Conf Ser Mater Sci Eng.* 2021;1116:012178.

58. Ledari SA, Milani JM, Lanbar FS. Improving gelatin-based emulsion films with cold plasma using different gases. *Food Sci Nutr*. 2020;8:6487–96.
59. Chichti E, Henrion G, Cleymand F, Jamshidian M, Linder M, Arab-Tehrany E. Effects of Ar-N<sub>2</sub>-O<sub>2</sub> microwave plasma on poly-L-lactic acid thin films designed for tissue engineering. *Plasma Process Polym*. 2013;10:535–43.
60. Pohan G, Chevallier P, Anderson DEJ, Tse JW, Yao Y, Hagen MW, et al. Luminal plasma treatment for small diameter polyvinyl alcohol tubular scaffolds. *Front Bioeng Biotechnol*. 2019;7:117.
61. Yang J, Bei J, Wang S. Improving cell affinity of poly(D,L-lactide) film modified by anhydrous ammonia plasma treatment. *Polym Adv Technol*. 2002;13:220–6.
62. Davoodi A, Zadeh HH, Joupari MD, Sahebalzamani MA, Khani MR, Shahabi S. Physicochemical- and biocompatibility of oxygen and nitrogen plasma treatment using a PLA scaffold. *AIP Adv*. 2020;10:125205.
63. Prasertsung I, Kanokpanont S, Mongkolnavin R, Wong CS, Panpranot J, Damrongsakkul S. Comparison of the behavior of fibroblast and bone marrow-derived mesenchymal stem cell on nitrogen plasma-treated gelatin films. *Mater Sci Eng C*. 2013;33:4475–9.
64. Jacobs T, Morent R, De Geyter N, Dubruel P, Leys C. Plasma surface modification of biomedical polymers: influence on cell-material interaction. *Plasma Chem Plasma Process*. 2012;32:1039–73.
65. Solouk A, Cousins BG, Mirzadeh H, Seifalian AM. Application of plasma surface modification techniques to improve hemocompatibility of vascular grafts: a review. *Biotechnol Appl Biochem*. 2011;58:311–27.
66. Farndale RW, Sixma JJ, Barnes MJ, de Groot PG. The role of collagen in thrombosis and hemostasis. *J Thromb Haemost*. 2004;2:561–73.
67. Keuren JF, Wielders SJ, Driessen A, Verhoeven M, Hendriks M, Lindhout T. Covalently-bound heparin makes collagen thromboresistant. *Arterioscler Thromb Vasc Biol*. 2004;24:613–7.
68. Niu Y, Galluzzi M. Hyaluronic acid/collagen nanofiber tubular scaffolds support endothelial cell proliferation, phenotypic shape and endothelialization. *Nanomaterials*. 2021;11:2334.
69. Brown M, Li J, Moraes C, Tabrizian M, Li-Jessen NYK. Decellularized extracellular matrix: new promising and challenging biomaterials for regenerative medicine. *Biomaterials*. 2022;289:121786.
70. Zhang X, Chen X, Hong H, Hu R, Liu J, Liu C. Decellularized extracellular matrix scaffolds: recent trends and emerging strategies in tissue engineering. *Bioact Mater*. 2022;10:15–31.
71. Copes F, Pien N, Van Vlierberghe S, Boccafoschi F, Mantovani D. Collagen-based tissue engineering strategies for vascular medicine. *Front Bioeng Biotechnol*. 2019;7:166.